Properties of Dopamine Release and Uptake in the Songbird Basal Ganglia

Samuel D. Gale and David J. Perkel

J Neurophysiol 93:1871-1879, 2005. First published Nov 17, 2004; doi:10.1152/jn.01053.2004

J Neurophysiol 93: 1871–1879, 2005.
First published November 17, 2004; doi:10.1152/jn.01053.2004.

Properties of Dopamine Release and Uptake in the Songbird Basal Ganglia

Samuel D. Gale[1] and David J. Perkel[2]

[1]*Graduate Program in Neurobiology and Behavior and* [2]*Departments of Biology and Otolaryngology, University of Washington, Seattle, Washington*

Submitted 6 October 2004; accepted in final form 10 November 2004

Gale, Samuel D. and David J. Perkel. Properties of dopamine release and uptake in the songbird basal ganglia. *J Neurophysiol* 93: 1871–1879, 2005. First published November 17, 2004; doi:10.1152/jn.01053.2004. Vocal learning in songbirds requires a basal ganglia circuit termed the anterior forebrain pathway (AFP). The AFP is not required for song production, and its role in song learning is not well understood. Like the mammalian striatum, the striatal component of the AFP, Area X, receives dense dopaminergic innervation from the midbrain. Since dopamine (DA) clearly plays a crucial role in basal ganglia–mediated motor control and learning in mammals, it seems likely that DA signaling contributes importantly to the functions of Area X as well. In this study, we used voltammetric methods to detect subsecond changes in extracellular DA concentration to gain better understanding of the properties and regulation of DA release and uptake in Area X. We electrically stimulated Ca^{2+}- and action potential–dependent release of an electroactive substance in Area X brain slices and identified the substance as DA by the voltammetric waveform, electrode selectivity, and neurochemical and pharmacological evidence. As in the mammalian striatum, DA release in Area X is depressed by autoinhibition, and the lifetime of extracellular DA is strongly constrained by monoamine transporters. These results add to the known physiological similarities of the mammalian and songbird striatum and support further use of voltammetry in songbirds to investigate the role of basal ganglia DA in motor learning.

INTRODUCTION

The neurotransmitter dopamine (DA) plays an important role in the function of basal ganglia circuits in motor control and learning. One such circuit is the anterior forebrain pathway (AFP) in songbirds, which is required for song learning in juveniles and plasticity of adult song but not for song production (Bottjer et al. 1984; Brainard and Doupe 2000; Scharff and Nottebohm 1991; Sohrabji et al. 1990; Williams and Mehta 1999). The first component of the AFP is the basal ganglia nucleus Area X. Like the mammalian striatum, Area X receives glutamatergic projections from pallial areas (the premotor nucleus HVC, used as a proper name, and the AFP output nucleus the lateral magnocellular nucleus of the anterior nidopallium, LMAN; nomenclature following Reiner et al. 2004) and a dense dopaminergic projection from the midbrain ventral tegmental area (VTA; Fig. 1; Bottjer 1993; Lewis et al. 1981). The essential role of the AFP in song learning and adult song plasticity and the known functions of basal ganglia DA in motor control and learning in mammals lead to the hypothesis that DA may play a key part in the song learning process or other functions of Area X. Consistent with an important role for DA in information processing in Area X, DA modulates the excitability of the major cell type (the spiny neuron) in Area X and also the strength of excitatory synaptic inputs to these cells (Ding and Perkel 2002, 2004; Ding et al. 2003).

In mammals, DA neurons fire spontaneously at a slow rate and transiently burst in response to salient events such as reward or reward predicting stimuli (Hyland et al. 2002; Schultz 1998). Burst firing enhances accumulation of extracellular DA (Chergui et al. 1994) and presumably causes the phasic increases in extracellular DA concentration observed in the striatum of behaving rats (Cheer et al. 2004; Phillips et al. 2003; Robinson et al. 2002; Roitman et al. 2004). Ultimately, the dynamics of extracellular DA concentration depends critically on local factors that vary among different regions of the brain: the density of DA release sites, the rate of DA uptake through transporter proteins, and the state of release-regulating neurotransmitter receptors on DA axon terminals. These factors influence whether DA acts via phasic (subsecond) signaling, slower fluctuations and/or by tonic influence on DA receptors.

A method of selectively measuring DA release with subsecond temporal resolution seems imperative for understanding the properties and functions of DA signaling in the songbird basal ganglia. In mammals, such measurements have been achieved in brain slices and in vivo using voltammetric methods in which endogenously released DA is oxidized on the surface of a carbon fiber, and the resulting current is recorded (reviewed in Robinson et al. 2003). We applied these techniques to songbirds to determine whether we could reliably measure DA release in Area X and if the factors regulating the extracellular concentration of DA are similar in the mammalian and songbird striatum. From brain slices of Area X, we electrically stimulated Ca^{2+}- and action potential–dependent release of an electroactive substance identified as dopamine by the shape of the voltammetric waveform, electrode selectivity, and by anatomical, neurochemical, and pharmacological evidence. The properties and regulation of DA release and uptake in Area X are similar to those reported previously in the mammalian striatum. These results extend the wealth of existing physiological and anatomical evidence for a high degree of similarity between avian and mammalian basal ganglia and verify that voltammetry will be a useful technique to measure DA release with high temporal resolution in Area X of songbirds in vivo.

METHODS

Care of birds and preparation of brain slices

All procedures were approved by the University of Washington Institutional Animal Care and Use Committee. Adult (>90 days old) male

Address for reprint requests and other correspondence: Samuel D. Gale, Univ. of Washington, Dept. of Otolaryngology, Box 356515, Seattle, WA 98195 (E-mail: samgale@u.washington.edu).

The costs of publication of this article were defrayed in part by the payment of page charges. The article must therefore be hereby marked "*advertisement*" in accordance with 18 U.S.C. Section 1734 solely to indicate this fact.

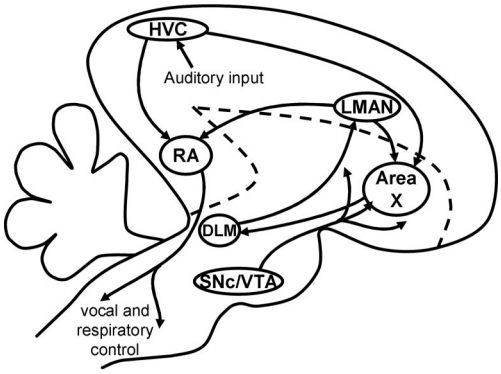

FIG. 1. Simplified diagram of the song system. HVC (used as a proper name) projects to the robust nucleus of the arcopallium (RA) as part of the motor pathway for song production. HVC also projects to RA indirectly via the anterior forebrain pathway, which includes Area X, the medial portion of the dorsolateral nucleus of the anterior thalamus (DLM), and the lateral magnocellular nucleus of the anterior nidopallium (LMAN). Dopaminergic inputs to Area X originate in the ventral tegmental area (VTA).

zebra finches were obtained from commercial suppliers and housed in groups of five or fewer on a 13/11-h light/dark cycle. Food and water were available at all times. Brain slices were prepared as described in detail by Stark and Perkel (1999). Birds were anesthetized with isoflurane and decapitated. The brain was removed and immersed in an ice-cold solution containing (in mM) 119 NaCl, 2.5 KCl, 1.3 $MgSO_4$, 1 NaH_2PO_4, 16.2 $NaHCO_3$, 2.5 $CaCl_2$, 11 D-glucose, and 10 HEPES. Coronal or parasagittal slices 300–400 μm thick were cut with a vibrating microtome. Slices were stored in artificial cerebrospinal fluid (ACSF), which was made of the same components described above for the slicing solution except for replacement of HEPES with an additional 10 mM $NaHCO_3$. The ACSF was initially ~35°C when the slices were transferred and allowed to cool to room temperature. All solutions were continuously bubbled with a gas mixture of 95% O_2-5% CO_2. Slices were left for at least 1 h before use.

Electrochemical recordings

To construct carbon fiber electrodes (CFEs), a single carbon fiber (15 mm long, 11 μm diam; P-25, Amoco, Tustin, CA) was inserted into the small end of a standard plastic P200 pipette tip. The plastic around the carbon fiber was melted with a heating coil in such a way that the pipette tip could be pulled by hand to a shank that sealed around the carbon fiber. The exposed carbon fiber tip was cut to a length of 30–50 μm by hand with a scalpel blade. The electrode was filled with 2 M KCl.

For recordings, slices were submerged in a small, illuminated chamber and perfused (2–3 ml/min) with ACSF warmed to 32°C. The borders of Area X were clearly visible through a dissecting microscope. The tip of the CFE was gently lowered into the slice to a depth of 50–150 μm. A bipolar, stainless steel stimulating electrode was inserted about 100 μm from the CFE. DA release was elicited by single 0.1-ms shocks (60–70 V amplitude) controlled by a stimulus isolation unit (Isoflex, AMPI, Jerusalem, Israel). Signals were amplified with a MultiClamp 700A amplifier in voltage-clamp mode and digitized with a Digidata 1322A (Axon Instruments, Foster City, CA). The electrode potential, stimulation, and data acquisition were controlled using Clampex 9.0 software (Axon Instruments). For constant potential amperometry (CPA), the CFE was held at +0.4 V; signals were low-pass filtered at 100 Hz and sampled at 10 kHz. For fast-scan cyclic voltammetry (FCV), the CFE was held at −0.4 V and a triangular waveform (−0.4 to 1 V and back at 300 V/s, a total of 9.33 ms) was applied every 100 ms (10 Hz); signals were low-pass filtered at 2 kHz and sampled at 20 kHz. Background-subtracted cyclic voltammograms (current-voltage plots) were made by subtracting the average of the current recorded for 10 voltammetric scans (1 s) prior to stimulation from the current recorded for each voltammetric scan after stimulation. Changes in DA concentration were quantified by plotting the peak oxidation current (converted to DA concentration as described below) of the voltammograms corresponding to each 100 ms-spaced time-point after stimulation. Data were analyzed and plotted using Clampfit 9.0 (Axon Instruments) and IGOR (Wave Metrics, Lake Oswego, OR).

CFEs were calibrated (at the end of a day of experiments) to convert current to approximate DA concentration. The CFE tip was carefully lowered into the end of the glass tube (1.1 mm ID) from which fresh ACSF perfused the slice. A 5-s "pulse" of 1–5 μM DA or norepinephrine (NE) dissolved in oxygenated ACSF was allowed to pass through the perfusion tubing and over the CFE, and the current change was recorded with CPA or FCV. CPA calibration without attempting to mimic the extracellular ascorbic acid concentration in brain tissue typically underestimates the sensitivity of the electrode by an order of magnitude (Kawagoe and Wightman 1994; Schmitz et al. 2001; Venton et al. 2002). Therefore only the peak oxidation current measured with FCV was used to estimate DA concentration in this paper, and CPA measurements are reported in units of current. Our CFEs were about three times more sensitive to DA than NE.

Slices were stimulated once every 2.5 min to allow full recovery from paired-pulse depression (see RESULTS and DISCUSSION). Drugs (diluted to their final concentration in the ACSF perfusing the slice chamber) were applied after the peak amplitude of the signal was stable for at least three consecutive stimulations.

For comparisons of peak DA release and decay time constant among Area X, medial striatum (MSt), and lateral striatum (LSt), DA release was recorded at 13 locations in the striatum of each parasagittal slice. Area X was divided into four quadrants to give four of the locations. Six locations were in the MSt outside of Area X (2 anterior, 1 ventral, and 3 posterior to Area X). Three locations were dorsal but not anterior to the globus pallidus and considered to be in the LSt. The CFE and stimulating electrodes were positioned at each location (in pseudorandom order) and DA release was evoked by single shock stimulation as described above. The peak amplitude of DA release and decay time constant were determined from a single trace taken after the amplitude was stable for three consecutive stimulations (as described for drug experiments above). The values of peak DA release and decay time constant at each location within a region (Area X, MSt, and LSt) were averaged to obtain a single value for each region in the slice. These are the values plotted and used for statistical analysis. DA uptake in the mammalian striatum is modeled according to Michaelis-Menten kinetics to determine the maximum rate of uptake (V_{max}). However, we do not know the value of K_m (binding affinity) for the DA transporter in birds or even whether just a single transporter contributes to DA decay in the zebra finch striatum. We instead fit the latter part of the decay phase (beginning at the concentration reached at the location with the smallest amplitude of DA release) to a single exponential to determine the decay time constant (see Fig. 5*A*).

Measurement of monoamine tissue content

For tissue content measurements, a 400- to 500-μm-thick coronal slice within the anterior and posterior borders of Area X was prepared as described above. While the slice was still immersed in the ice-cold slicing solution, a square piece of tissue within the medial-lateral and dorsal-ventral borders of Area X was dissected with a sharp scalpel under a dissecting microscope. The dissected piece of tissue was transferred to a plastic tube and frozen on dry ice. A similar-sized piece of tissue was cut from the pallium dorsal to Area X in the same slice. Tissue samples remained frozen at −80°C or on dry ice until analyzed for monoamine content. Monoamine levels were measured by HPLC with electrochemical detection at the Neurochemistry Core Lab in Vanderbilt University's Center for Molecular Neuroscience

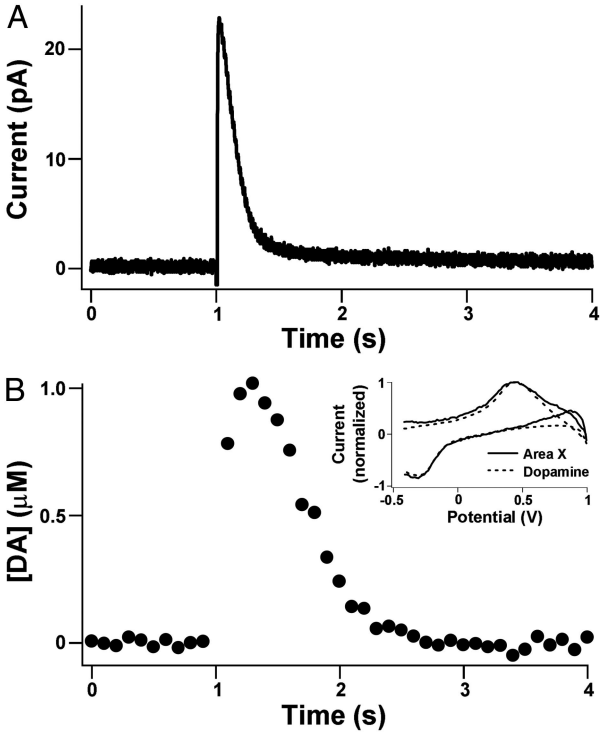

FIG. 2. Examples of dopamine (DA) release measured after single-shock stimulation in Area X slices with constant potential amperometry (CPA) (*A*) and fast-scan cyclic voltammetry (FCV) (*B*). Stimulation occurred at 1 s. Example cyclic voltammograms are shown in the *inset* of *B* for DA release in Area X (solid line) and for exogenous DA during calibration (dashed line).

(http://www.mc.vanderbilt.edu/root/vumc.php?site=neurosci&doc=697) and are reported as amount of monoamine (ng) per amount of total protein (mg) in the tissue sample.

Statistics

Prism 3.0 (Graph Pad Software, San Diego, CA) was used for statistical testing with the tests indicated in RESULTS and DISCUSSION. All tests were two-tailed. $P < 0.05$ was considered significant. Values of n for a given experiment indicate number of slices, and no more than two slices from a single bird were used for the same type of experiment.

Drugs

Atropine, baclofen, carbachol, $CdCl_2$, clonidine, desipramine, DA, fluvoxamine, GBR-12935, mecamylamine, nicotine, nomifensine, NE, pargyline, quinpirole, TTX, and yohimbine were purchased from Sigma (St. Louis, MO). (1S,3R)-1-aminocyclopentane-1,3-dicarboxylic acid (APCD), (RS)-3,5-dihydroxyphenylglycine (DHPG), maprotiline, pilocarpine, and sulpiride were purchased from Tocris (Ellisville, MO).

RESULTS AND DISCUSSION

Measurement and identification of synaptic DA release

A single shock from a stimulating electrode positioned near a CFE held at constant potential (0.4 V) in Area X reliably caused a rapid rise in current well above noise that generally decayed back to baseline in <1 s (Fig. 2*A*). No response was observed when the CFE was held at 0 V. Similar events recorded with FCV revealed a background-subtracted voltammogram (current-voltage curve) similar to the voltammogram obtained from DA or NE dissolved in ACSF (Fig. 2*B, inset*). The current at the peak oxidation potential measured with FCV changed with a time course similar to the current change measured with CPA (Fig. 2*B*). However, the time to peak and the decay of the FCV signal were slightly slower than those of the CPA signal because of adsorption of analyte to the CFE between FCV scans (Bath et al. 2000; Venton et al. 2002).

The shape of the voltammogram strongly suggested we were measuring release of DA and/or NE (DA and NE produce very similar voltammograms). In mammals, it is commonly assumed that CFEs solely measure DA, and not NE, release in the striatum because CFEs are about three times more sensitive to DA than NE (see METHODS) and the density of DA innervation and DA tissue content are much greater than those of NE in the striatum (DA:NE content is 100:1 in the caudate and 10:1 in the nucleus accumbens of rats; Garris et al. 1993; Kuhr et al. 1986). Similarly, in zebra finches, the tyrosine hydroxylase (TH; the rate-limiting enzyme in the synthesis of both DA and NE) positive fibers that project heavily to Area X originate from cell bodies in VTA that are TH positive but not positive for dopamine-β-hydroxylase (DβH; an enzyme involved in conversion of DA to NE and thus a marker of noradrenergic neurons), and lesions of VTA completely abolish catecholamine histofluorescence in Area X (Bottjer 1993; Lewis et al. 1981; Mello et al. 1998). DβH-positive fibers are sparse in Area X and surrounding striatal areas (Mello et al. 1998). We directly measured monoamine content in tissue homogenate from Area X and from pallium located dorsal to Area X (a region with much lighter TH immunostaining) using liquid chromatography. Levels of NE, serotonin (5-hydroxytryptamine, or 5-HT), and the 5-HT metabolite 5-hydroxyindole-3-acetic acid (5-HIAA) were not significantly different in Area X and pallium ($P > 0.4$, paired t-test), whereas, as expected, levels of DA and its metabolites dihydroxyphenylacetic acid (DOPAC) and homovanillic acid (HVA) were significantly greater in Area X than in pallium ($P < 0.05$; Fig. 3). DA was on average 40 times more abundant than NE in Area X ($P < 0.0001$, paired t-test; Fig. 3). This result is qualitatively the same as that of Harding et al. (1998), who found DA was about five times more abundant than NE in Area X in 90-day old zebra finches (the difference in absolute amounts of DA and NE measured here and by Harding et al. might be due to differences in release and metabolism of catecholamines while handling the bird or during tissue collection). Thus the zebra finch striatum seems to receive, like the striatum of mammals and other

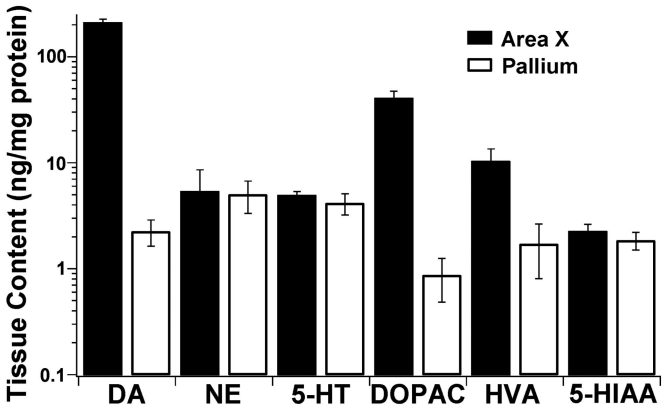

FIG. 3. Mean tissue content of DA, NE, 5-HT, and the metabolites DOPAC, HVA, and 5-HIAA from Area X (solid bars) and pallium located dorsal to Area X (open bars) from 6 adult zebra finches. Error bars represent SE.

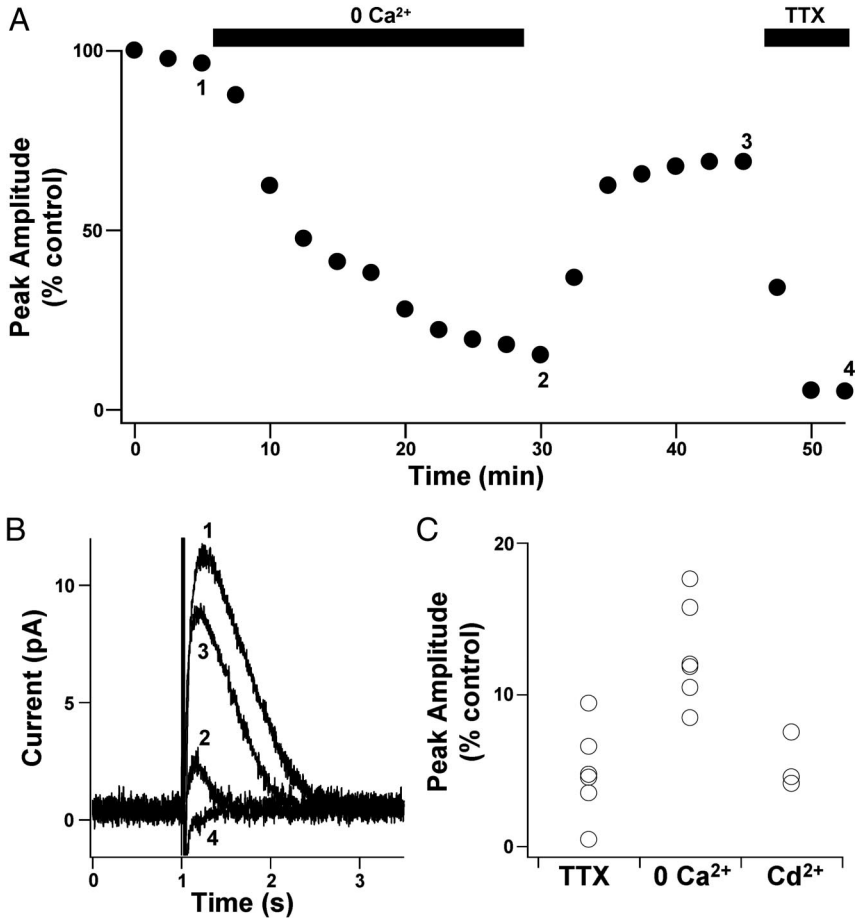

FIG. 4. *A*: example of an experiment showing effect of removing extracellular Ca^{2+} (0 Ca^{2+}) or applying TTX on DA release. *B*: CPA traces from the time-points indicated in *A*. Stimulation occurred at 1 s. *C*: inhibition of DA release in all experiments with TTX ($n = 6$), 0 Ca^{2+} ($n = 6$), and Cd^{2+} ($n = 3$).

birds (Reiner et al. 1994), a very dense DA innervation and a relatively sparse noradrenergic innervation. Although tissue content is only a measure of what may potentially be released by local stimulation in brain slices (for instance, it does not distinguish between neurotransmitter in the releasable pool of vesicles versus storage pools; Garris and Wightman 1994), the higher sensitivity of CFEs for DA than NE, anatomical data, and relative amounts of DA and NE contained in Area X suggest that the CPA and FCV signals resulting from electrical stimulation in Area X are a measure of DA release and that NE is unlikely to make more than a small contribution to these signals.

To ask whether the DA release we evoked is dependent on action potentials and Ca^{2+} entry, we used CPA to measure the peak amplitude of DA release after blocking action potentials with TTX (2 μM), preventing Ca^{2+} entry by removing Ca^{2+} from the ACSF bathing the slice, or blocking voltage-gated Ca^{2+} channels with Cd^{2+} ions (100 μM $CdCl_2$). TTX ($n = 6$), removal of extracellular Ca^{2+} ($n = 6$), or Cd^{2+} ($n = 3$) all significantly reduced the peak amplitude of evoked DA release by 80–100% ($P < 0.001$, *t*-test), and the effects of Ca^{2+} removal and Cd^{2+} were at least partially reversible (Fig. 4). Thus, in Area X as in mammalian striatal slices, local electrical stimulation elicits Ca^{2+}- and action potential–dependent release of DA.

Regional comparison of DA release and uptake in the avian striatum

The peak DA concentration measured at the CFE depends on the density of DA release sites, the amount of DA released at each site, and the distance DA diffuses from each release site (largely controlled by the rate of DA uptake through transporters). Peak DA release and the rate of DA uptake thus reflect important properties of DA signaling and vary across different regions of the mammalian brain. For instance, in rats, peak DA release is greater and DA uptake rate faster by an order of magnitude in the striatum than in the prefrontal cortex and amygdala (Garris and Wightman 1994). Also, in both the rodent and primate striatum, peak DA release tends to be greater and uptake faster in "motor" compared with "limbic" striatal subregions (Cragg 2003; Cragg et al. 2000, 2002; Garris and Wightman 1994; Jones et al. 1995, 1996). To determine whether peak DA release and the kinetics of DA uptake are different among Area X and other parts of zebra finch striatum, we recorded DA release in response to a single shock in three different regions of the striatum (Area X, MSt outside of Area X, and LSt) in parasagittal slices ($n = 8$; see METHODS). FCV was used so that we could compare peak release amplitude in terms of estimated concentration (see METHODS). To compare rate of DA uptake, we fit the latter part of the decay phase to a single exponential and measured the time constant (see METHODS and Fig. 5*A*). Peak DA concentration after a single shock varied from about 0.5 to 2.5 μM (similar to concentrations observed in mammalian striatal slices) and was significantly greater in Area X than MSt and LSt ($P < 0.05$, repeated measures ANOVA and Tukey's multiple comparisons test; Fig. 5*B*). This is consistent with the greater intensity of TH-expressing fibers (and thus probably

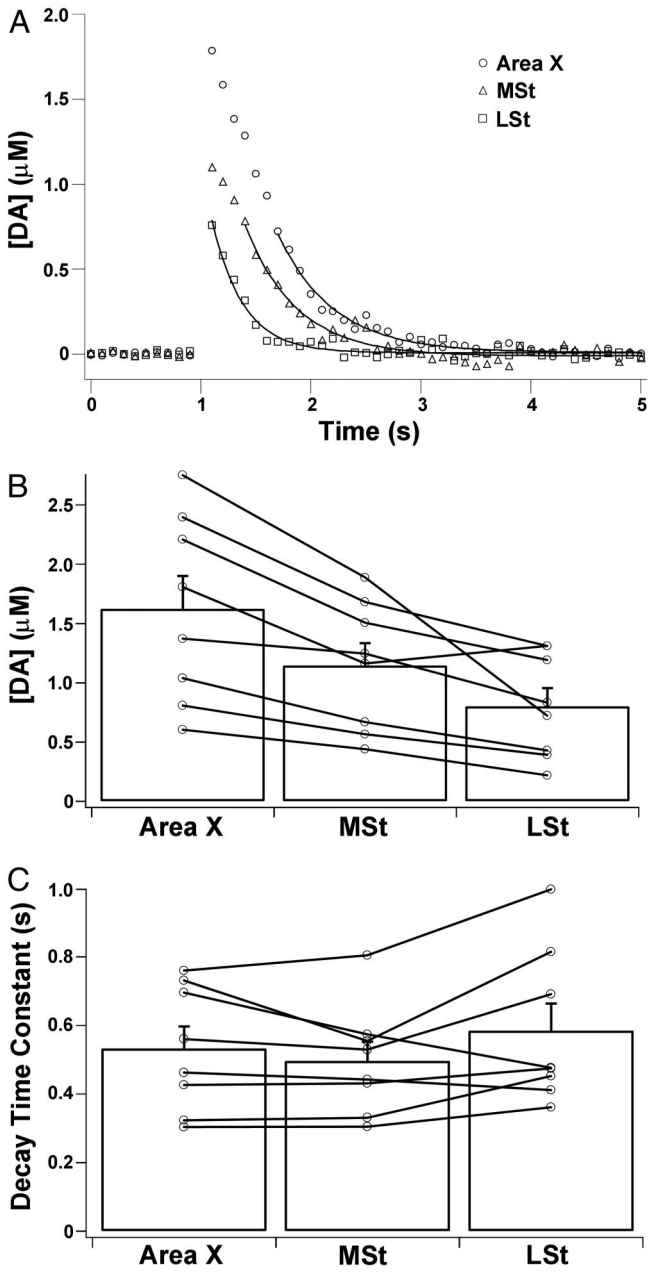

FIG. 5. *A*: example FCV recordings from Area X (circles), MSt outside of Area X (triangles), and LSt (squares). Stimulation occurred at 1 s. Latter parts of the decay phase are fit to a single exponential (shown with solid lines) beginning at the same concentration (see METHODS). *B*: peak DA release in the Area X, medial striatum (MSt), and lateral striatum (LSt) are plotted as open circles and are connected by lines for measurements made in the same slice ($n = 8$). Mean value for each area is indicated by an open bar. Error bars represent SE. *C*: decay time constants in Area X, MSt, and LSt plotted as in *B*.

denser release sites) in Area X than surrounding striatum in adult zebra finches (Soha et al. 1996). Greater fiber density might also result in a greater density of monoamine transporters and thus faster uptake of DA in Area X, but the decay time constant was not significantly different among Area X, MSt, and LSt ($P = 0.38$, repeated measures ANOVA; Fig. 5*C*).

Regulation of DA uptake through monoamine transporters

In mammals, DA is rapidly diluted as it diffuses from the release site, and thereafter, the time and distance DA travels and interacts with receptors is heavily influenced by the rate of uptake via the DA transporter (DAT) (Cragg and Rice 2004). To assay the influence of monoamine transporters on DA transmission in Area X, we measured (with CPA) the half-life (time to 50% decay) of DA released by a single shock in the presence of monoamine uptake transporter inhibitors. The DAT inhibitors GBR-12935 (GBR; 5 μM, $n = 6$) and nomifensine (5 μM, $n = 5$) increased the half-life of DA released in Area X by over 350%, indicating that DA transmission is tightly controlled by uptake through the DAT in Area X (both effects $P < 0.05$, *t*-test; Fig. 6). Surprisingly, the NE transporter (NET) inhibitors desipramine (1 μM, $n = 6$) and maprotiline (10 μM, $n = 5$) at concentrations that are specific to NET in mammals also substantially increased the half-life of DA released in Area X (by over 800 and 300%, respectively; both effects $P < 0.01$, *t*-test; Fig. 6).

Expression of DAT or NET is specific to the cells that synthesize and release the corresponding neurotransmitter in mammals; however, both DAT and NET can transport either catecholamine (reviewed in Torres et al. 2003). The NET (located on NE-releasing axons) has a significant role in the uptake of DA in the rat prefrontal cortex, where DA innervation is sparse compared with the striatum and DAT expression is low (Moron et al. 2002; Mundorf et al. 2001; Sesack et al. 1998). The NET does not contribute to DA uptake in the mammalian striatum (Cragg 2003; Cragg et al. 2000, 2002; Jones et al. 1995, 1996). Even in the nucleus accumbens shell, where there is moderate NE innervation and expression of NET and where DAT expression is less dense compared with the dorsal striatum and nucleus accumbens core, NET inhibitors do not affect DA uptake in normal or DAT knock-out mice (Berridge et al. 1997; Budygin et al. 2002; Delfs et al. 1998; Nirenberg et al. 1997; Schroeter et al. 2000). Hence, the possibility that NET located on NE axons contributes strongly to DA uptake in Area X seems unlikely given the very high-density of DA fibers compared with NE fibers. Another possibility is that DA axons in Area X express two transporters—one pharmacologically DAT-like and the other NET-like—that both contribute significantly to DA uptake. If either of the possibilities stated above were true, the combination of a DAT inhibitor and NET inhibitor might have greater effect on DA half-life in Area X than either of the drugs alone. Co-application of GBR and desipramine ($n = 5$) or GBR and maprotiline ($n = 5$) had no further effect on DA half-life than desipramine or maprotiline alone ($P = 0.28$ and $P = 0.93$, respectively, unpaired *t*-test; Fig. 6), suggesting instead that both types of drugs (DAT and NET inhibitors) act on the zebra finch DAT. These results show that the spatial and temporal influence of DA in Area X, as in the mammalian striatum, are strongly restricted by the action of DA transporters.

The 5-HT transporter (SERT) inhibitor fluvoxamine (5 μM, $n = 5$) and the monoamine oxidase (MAO-B) inhibitor pargyline (20 μM, $n = 3$) had no effect on DA half-life in Area X ($P = 0.86$ and 0.53, respectively, *t*-test; Fig. 6). This is consistent with our other evidence (most importantly, the shape of the voltammogram) that 5-HT and DOPAC do not contribute to our CPA and FCV measurements and shows that SERT and MAO-B are not involved in the rapid decay of extracellular DA in Area X.

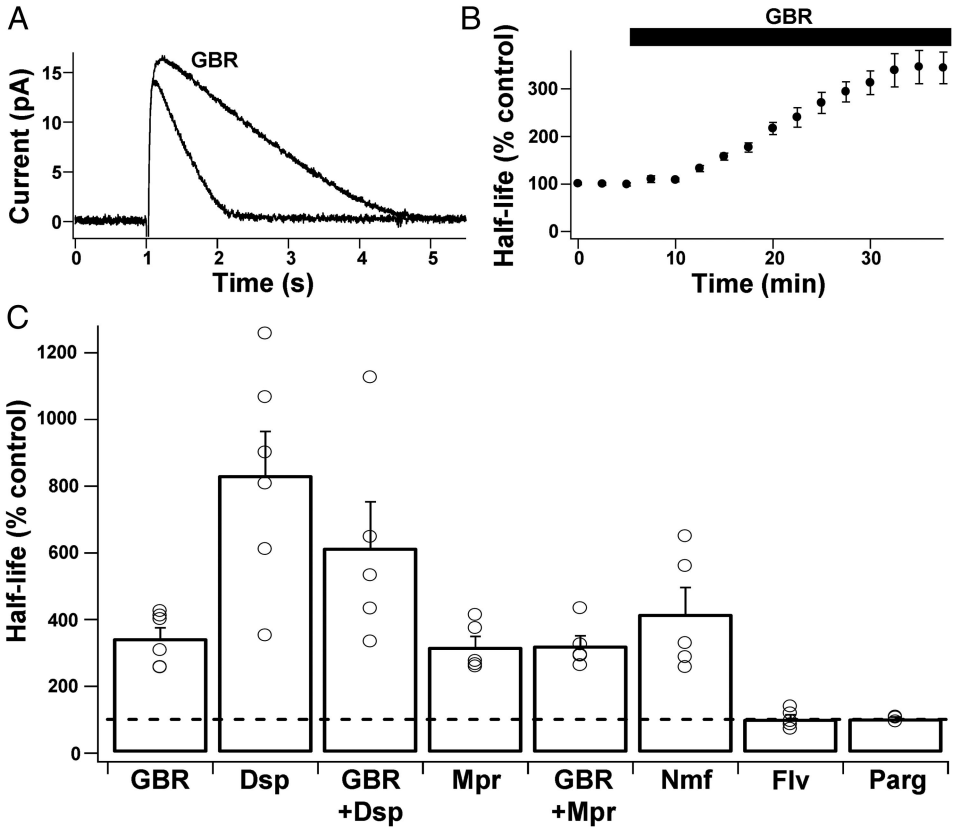

FIG. 6. *A*: example CPA traces before and after applying the DA transporter (DAT) inhibitor GBR. Stimulation occurred at 1 s. *B*: time course of the effect of GBR averaged over 6 experiments. Error bars represent SE. *C*: change in half-life of released DA after application of GBR ($n = 6$), desipramine [Dsp, $n = 6$, NE transporter (NET) inhibitor], GBR and desipramine ($n = 5$), maprotiline (Mpr, $n = 5$, NET inhibitor), GBR and maprotiline ($n = 5$), nomifensine (Nmf, $n = 5$, DAT inhibitor), fluvoxamine (Flv, $n = 5$, SERT inhibitor), and pargyline (Parg, $n = 3$, MAO-B inhibitor). Individual experiments are plotted with circles. Mean for each group is shown with an open bar, and error bars represent SE. Dashed line indicates 100%.

Control of DA release by presynaptic neurotransmitter receptors

In mammals, extracellular DA inhibits its own release by binding to D2 receptors on DA axon terminals. We tested the effect of the D2 agonist quinpirole (10 μM) and D2 antagonist sulpiride (10 μM) on the peak amplitude of DA release in Area X recorded with CPA. Since DA can activate α2 noradrenergic receptors (Cornil et al. 2002; Zhang et al. 1999) and α2 receptor agonists reduce DA release in the mammalian striatum (Trendelenburg et al. 1994; Yavich et al. 1997), we also tested the possibility that α2 receptors can act as release-regulating autoreceptors on DA terminals in Area X using the α2 receptor agonist clonidine (10 μM) and antagonist yohimbine (10 μM). Quinpirole decreased DA release by ~50% ($n = 5$, $P < 0.0001$, *t*-test; Fig. 7). The effect of quinpirole was significantly reduced by sulpiride ($n = 5$; $P < 0.001$, 1-way ANOVA with Tukey's multiple comparisons test) and was not affected by yohimbine ($n = 3$, $P > 0.05$, same test); a small (<10%) but significant effect of quinpirole on DA release persisted in the presence of sulpiride ($n = 5$, $P < 0.001$, *t*-test). Sulpiride itself increased DA release by ~35% ($n = 7$, $P < 0.01$, *t*-test), suggesting that D2 receptors are tonically active and inhibiting DA release in our slice preparation. Tonic D2 activation in our slice preparation might be the result of constitutive DA release that is independent of the activity of DA cell bodies, which were not present in our slices. Clonidine decreased DA release by ~25% ($n = 6$, $P < 0.001$, *t*-test). The effect of clonidine was blocked by yohimbine ($n = 3$, $P < 0.01$, 1-way ANOVA with Tukey's multiple comparisons test) but not by sulpiride ($n = 3$, $P > 0.05$). The block of clonidine by yohimbine was complete ($n = 3$, $P = 0.38$, *t*-test). Yohimbine alone had no effect on DA release in Area X ($n = 6$, $P = 0.56$, *t*-test).

These results indicate that DA release in Area X is inhibited by activation of D2 and α2 receptors. To determine whether endogenously released DA can activate these receptors and inhibit further DA release (autoinhibition), we measured (with CPA) the ratio of the peak amplitude of DA release caused by single shocks separated by short time intervals (the paired-pulse ratio, or PPR) in normal conditions and in the presence of sulpiride or yohimbine at the same recording position. For intervals close enough that the second release event occurred during the decay of DA released from the first shock, the amplitude of the second release event was determined by subtracting the record of DA release caused by a single pulse from the two-pulse record (Cragg 2003; Phillips et al. 2002). In control conditions, there was a time-dependent paired-pulse depression (PPD) of DA release in Area X (maximum ~80% depression at 1 s; Fig. 8, *A* and *B*). Sulpiride ($n = 5$) or yohimbine ($n = 5$) partially decreased the magnitude of PPD (sulpiride 3 times more so than yohimbine), suggesting that DA release in Area X inhibits its own release by activating D2 and, more modestly, α2 receptors. The effect of sulpiride on the PPR was significant ($P < 0.05$, paired *t*-test) for the intervals from 0.1 and 3 s, and that of yohimbine for the intervals from 0.05 to 1 s. To determine the time course and magnitude of autoinhibition mediated by D2 and α2 receptors, we subtracted the PPR measured for each interpulse interval under control conditions from the PPR at the same intervals measured after sulpiride or yohimbine application (Fig. 8*C*). D2 receptor–mediated autoinhibition was activated within 50 ms of the first stimulation pulse, reached a maximum at 500 ms

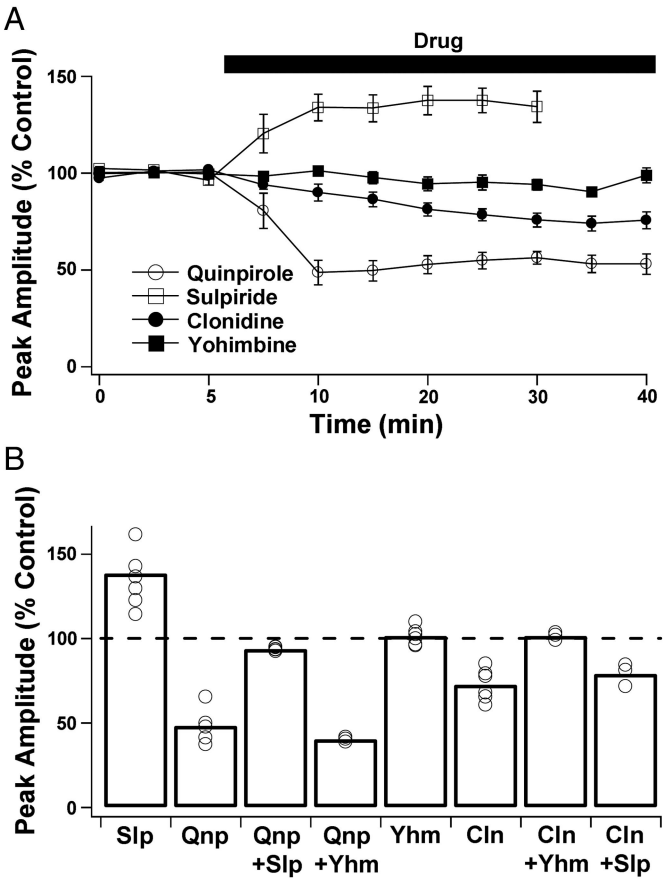

FIG. 7. *A*: average time course of the effects of quinpirole (D2 agonist, open circles, $n = 5$), sulpiride (D2 antagonist, open squares, $n = 7$), clonidine (α2 agonist, filled circles, $n = 6$), and yohimbine (α2 antagonist, filled squares, $n = 6$). Error bars indicate SE. *B*: change in peak amplitude of DA release after application of sulpiride (Slp, $n = 7$), quinpirole (Qnp, $n = 5$), quinpirole in the presence of sulpiride ($n = 5$), quinpirole in the presence of yohimbine (Yhm, $n = 3$), yohimbine ($n = 6$), clonidine (Cln, $n = 6$), clonidine in the presence of yohimbine ($n = 3$), and clonidine in the presence of sulpiride ($n = 3$). Individual experiments are plotted with circles. Mean for each group is shown with an open bar.

(accounting for ≤30% of the PPD), and terminated by about 5 s after the initial pulse. The time course and magnitude of D2-mediated autoinhibition measured in Area X slices are similar to measurements in mammalian striatal slices (Phillips et al. 2002). Autoinhibition mediated by α2 receptors in Area X followed a similar time course but was weaker (accounting for no more than 10% of the PPD) and shorter lasting (<2 s). The difference in the magnitudes of the D2 and α2 receptor–mediated effects could be due to receptor numbers, efficiency of activation by DA, and intracellular signaling pathways used. The relative magnitude of the effect of evoked DA release on D2 and α2 receptors is also influenced by the fact that D2 receptors are already partially activated in the slice, whereas α2 receptors are not (Fig. 7).

What is the origin of the substantial D2/α2-independent component of the PPD? Release of other neurotransmitters besides DA by the first shock might contribute to time-dependent depression of subsequent DA release. Glutamate, GABA, and acetylcholine (ACh) can all modulate DA release in the mammalian striatum (Avshalumov et al. 2003; Rice and Cragg 2004; Schmitz et al. 2002; Zhang and Sulzer 2003, 2004; Zhou

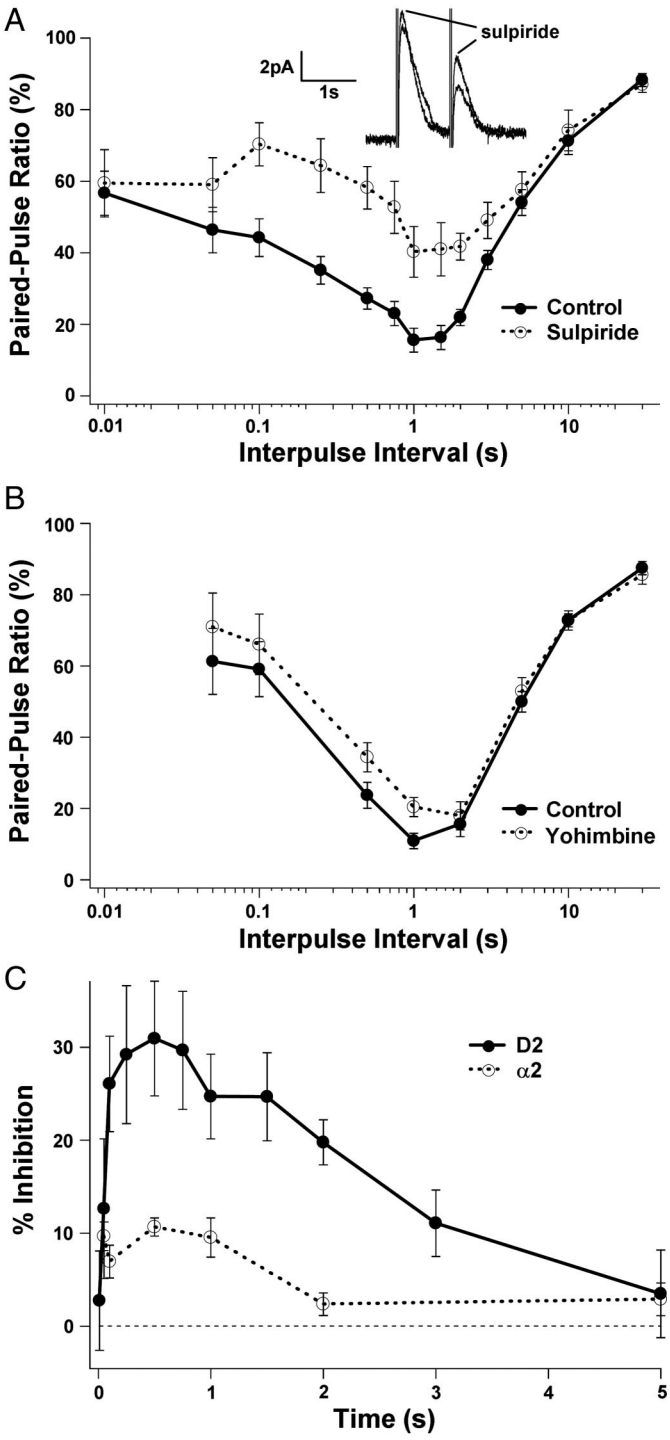

FIG. 8. *A*: paired-pulse ratio (PPR) of peak amplitude of DA release for various interpulse intervals in control conditions (filled circles) and (at the same recording position) in the presence of the D2 receptor antagonist sulpiride (open circles; $n = 5$). Error bars represent SE. *Inset*: example traces of DA release in response to paired stimulation (1-s interpulse interval) in the presence and absence of sulpiride. *B*: same as *A* except showing the PPR in control conditions (filled circles; different experiments from those in *A*) and in the presence of the α2 receptor antagonist yohimbine (open circles; $n = 5$). *C*: time course of D2 (filled circles) and α2 (open circles) receptor-mediated autoinhibition of DA release. Each point represents the PPR in control conditions subtracted from the PPR in the presence of drug. Error bars represent SE.

et al. 2001). Nicotine (10 μM, $n = 3$), the nicotinic receptor antagonist mecamylamine (10 μM, $n = 7$), the muscarinic receptor agonist pilocarpine (30 μM, $n = 3$) and antagonist atropine (20 μM, $n = 4$), and the nonspecific cholinergic agonist carbachol (20–100 μM, $n = 6$) all had no effect on the amplitude of DA released by a single shock in Area X (data not shown). Although spontaneously active cholinergic interneurons are present in brain slices of Area X (Carrillo and Doupe 2004; Farries and Perkel 2002), these results suggest that, unlike in mammals (Zhou et al. 2001), DA release is not regulated by tonic ACh release in Area X. However, these experiments do not definitively rule out the possibility that release-regulating nicotinic ACh receptors are present on DA axons in Area X. The group 1 metabotropic glutamate receptor (mGluR) agonist DHPG (100 μM, $n = 5$), the groups 1 and 2 mGluR agonist ACPD (100 μM, $n = 6$), and the $GABA_B$ receptor agonist baclofen (30 μM, $n = 7$) significantly reduced the amplitude of DA released by a single shock in Area X by 40 ± 9% (SD), 28 ± 11%, and 22 ± 11%, respectively ($P < 0.01$, *t*-test; data not shown). Activation of mGluR, $GABA_B$, or other receptors by endogenous neurotransmitter might contribute to the observed PPD. A portion of the autoinhibition-independent PPD might also be due to depletion of docked vesicles at DA synapses after local stimulation in brain slices. The slow, autoinhibition-independent PPD is less pronounced in vivo in mammals (Benoit Marand et al. 2001; Montague et al. 2004; Schmitz et al. 2003).

Summary and conclusions

We have shown that electrical stimulation in Area X from adult zebra finches results in Ca^{2+}- and action potential–dependent release of a substance identifiable as DA by the following electrochemical, anatomical, and pharmacological evidence.

1) The shape of the voltammogram obtained with FCV after electrical stimulation in Area X is identical to that of exogenous DA and known to be unique to DA and NE.

2) The CFEs used are three times more sensitive to DA than NE.

3) Area X receives a rich projection from neurons in VTA that synthesize DA but not NE.

4) The tissue content of DA is about 40 times more abundant than NE in Area X.

5) The half-life of the released substance is dramatically increased by drugs known to block the uptake of DA through proteins that transport DA.

6) The released substance inhibits its own release by activating D2 DA receptors with a time course similar to that of D2 receptor–mediated autoinhibition of DA release in mammalian striatal slices.

The factors shown to regulate release and uptake of DA in Area X are very similar to those reported for the mammalian striatum, suggesting a common functional design for DA neurotransmission in mammalian and songbird basal ganglia. Mammalian DA neurons spontaneously fire action potentials at a slow rate in vivo; uptake and tonic depression of release by D2 autoreceptors help set the steady-state extracellular concentration of DA in the striatum. During burst firing, DA released at short interspike intervals accumulates faster than uptake can remove it, resulting in a phasic increase in extracellular DA that reaches farther from the release site, has an increased probability of activating low-affinity receptors, and transiently reduces (via autoinhibition) subsequent DA release by the slow, tonic discharge of DA neurons. This amplification of extracellular DA in the striatum might be important for effectively transmitting the phasic signal represented by burst firing of DA neurons.

The temporal dynamics and function of DA signaling in behaving songbirds are not known. The results presented here lend confidence to the possibility of using voltammetry to measure changes in extracellular DA concentration with subsecond temporal resolution in Area X in vivo, although even more caution will be required in interpreting the identity of catecholamines contributing to voltammetric signals in vivo. Since DA plays such an important role in mammalian basal ganglia function, knowing the conditions that cause DA release and the cellular effects of DA in Area X will likely contribute to understanding how the AFP functions in songbirds, which may in turn prove useful as a model of basal ganglia function in general.

ACKNOWLEDGMENTS

We thank D.-S. Koh and B. Hille for help with making carbon fiber electrodes, P. Phillips for advice on voltammetry, and P. Phillips and A. Person for comments on previous versions of this paper.

GRANTS

This work was supported by National Institute of Mental Health Grant MH-066128 and a National Science Foundation Graduate Fellowship.

REFERENCES

Avshalumov MV, Chen BT, Marshall SP, Pena DM, and Rice ME. Glutamate-dependent inhibition of dopamine release in striatum is mediated by a new diffusible messenger, H_2O_2. *J Neurosci* 23: 2744–2750, 2003.

Bath BD, Michael DJ, Trafton BJ, Joseph JD, Runnels PL, and Wightman RM. Subsecond adsorption and desorption of dopamine at carbon-fiber microelectrodes. *Anal Chem* 72: 5994–6002, 2000.

Benoit Marand M, Borrelli E, and Gonon F. Inhibition of dopamine release via presynaptic D2 receptors: time course and functional characteristics in vivo. *J Neurosci* 21: 9134–9141, 2001.

Berridge CW, Stratford TL, Foote SL, and Kelley AE. Distribution of dopamine beta-hydroxylase-like immunoreactive fibers within the shell subregion of the nucleus accumbens. *Synapse* 27: 230–241, 1997.

Bottjer SW. The distribution of tyrosine hydroxylase immunoreactivity in the brains of male and female zebra finches. *J Neurobiol* 24: 51–69, 1993.

Bottjer SW, Miesner EA, and Arnold AP. Forebrain lesions disrupt development but not maintenance of song in passerine birds. *Science* 224: 901–903, 1984.

Brainard MS and Doupe AJ. Interruption of a basal ganglia-forebrain circuit prevents plasticity of learned vocalizations. *Nature* 404: 762–766, 2000.

Budygin EA, John CE, Mateo Y, and Jones SR. Lack of cocaine effect on dopamine clearance in the core and shell of the nucleus accumbens of dopamine transporter knock-out mice. *J Neurosci* 22: RC222, 2002.

Carrillo GD and Doupe AJ. Is the songbird Area X striatal, pallidal, or both? An anatomical study. *J Comp Neurol* 473: 415–437, 2004.

Cheer JF, Wassum KM, Heien ML, Phillips PE, and Wightman RM. Cannabinoids enhance subsecond dopamine release in the nucleus accumbens of awake rats. *J Neurosci* 24: 4393–4400, 2004.

Chergui K, Suaud-Chagny MF, and Gonon F. Nonlinear relationship between impulse flow, dopamine release, and dopamine elimination in the rat brain in vivo. *Neuroscience* 62: 641–645, 1994.

Cornil CA, Balthazart J, Motte P, Massotte L, and Seutin V. Dopamine activates noradrenergic receptors in the preoptic area. *J Neurosci* 22: 9320–9330, 2002.

Cragg SJ. Variable dopamine release probability and short-term plasticity between functional domains of the primate striatum. *J Neurosci* 23: 4378–4385, 2003.

Cragg SJ, Hille CJ, and Greenfield SA. Dopamine release and uptake dynamics within the nonhuman primate striatum in vitro. *J Neurosci* 20: 8209–8217, 2000.

Cragg SJ, Hille CJ, and Greenfield SA. Functional domains in dorsal striatum of the nonhuman primate are defined by the dynamic behavior of dopamine. *J Neurosci* 22: 5705–5712, 2002.

Cragg SJ and Rice ME. DAncing past the DAT at a DA synapse. *Trends Neurosci* 27: 270–277, 2004.

Delfs JM, Zhu Y, Druhan JP, and Aston-Jones GS. Origin of noradrenergic afferents to the shell subregion of the nucleus accumbens: anterograde and retrograde tract-tracing studies in the rat. *Brain Res* 806: 127–140, 1998.

Ding L and Perkel DJ. Dopamine modulates excitability of spiny neurons in the avian basal ganglia. *J Neurosci* 22: 5210–5218, 2002.

Ding L and Perkel DJ. Long-term potentiation in a avian basal ganglia nucleus essential for vocal learning. *J Neurosci* 24: 488–494, 2004.

Ding L, Perkel DJ, and Farries MA. Presynaptic depression of glutamatergic synaptic transmission by D1-like dopamine receptor activation in the avian basal ganglia. *J Neurosci* 23: 6086–6095, 2003.

Farries MA and Perkel DJ. A telenchephalic nucleus essential for song learning contains neurons with physiological characteristics of both striatum and globus pallidus. *J Neurosci* 22: 3776–3787, 2002.

Garris PA, Collins LB, Jones SR, and Wightman RM. Evoked extracellular dopamine in vivo in the medial prefrontal cortex. *J Neurochem* 61: 637–647, 1993.

Garris PA and Wightman RM. Different kinetics govern dopaminergic transmission in the amygdala, prefrontal cortex, and striatum: in vivo voltametric study. *J Neurosci* 14: 442–450, 1994.

Harding CF, Barclay SR, and Waterman SA. Changes in catecholamine levels and turnover rates in hypothalamic, vocal control, and auditory nuclei in male zebra finches during development. *J Neurobiol* 34: 329–346, 1998.

Hyland BI, Reynolds JN, Hay J, Perk CG, and Miller R. Firing modes of midbrain dopamine cells in the freely moving rat. *Neuroscience* 114: 475–492, 2002.

Jones SR, Garris PA, Kilts CD, and Wightman RM. Comparison of dopamine uptake in the basolateral amygdaloid nucleus, caudate-putamen, and nucleus accumbens of the rat. *J Neurochem* 64: 2581–2589, 1995.

Jones SR, O'Dell SJ, Marshall JF, and Wightman RM. Functional and anatomical evidence for different dopamine dynamics in the core and shell of the nucleus accumbens in slices of rat brain. *Synapse* 23: 224–231, 1996.

Kawagoe KT and Wightman RM. Characterization of amperometry for in vivo measurement of dopamine dynamics in the rat brain. *Talanta* 41: 865–874, 1994.

Kuhr WG, Bigelow JC, and Wightman RM. In vivo comparison of the regulation of releasable dopamine in the caudate nucleus and the nucleus accumbens of the rat brain. *J Neurosci* 6: 974–982, 1986.

Lewis JW, Ryan SM, Arnold AP, and Butcher LL. Evidence for a catecholaminergic projection to Area X in the zebra finch. *J Comp Neurol* 196: 347–354, 1981.

Mello CV, Pinaud R, and Ribeiro S. Noradrenergic system of the zebra finch brain: immunocytochemical study of dopamine-β-hydroxylase. *J Comp Neurol* 400: 207–228, 1998.

Montague PR, McClure SM, Baldwin PR, Phillips PEM, Budygin EA, Stuber GD, Kilpatrick MR, and Wightman RM. Dynamic gain control of dopamine delivery in freely moving animals. *J Neurosci* 24: 1754–1759, 2004.

Moron JA, Brockington A, Wise RA, Rocha BA, and Hope BT. Dopamine uptake through the norepinephrine transporter in brain regions with low levels of the dopamine transporter: evidence from knock-out mouse lines. *J Neurosci* 22: 389–395, 2002.

Mundorf ML, Joseph JD, Austin CM, Caron MG, and Wightman RM. Catecholamine release and uptake in the mouse prefrontal cortex. *J Neurochem* 79: 130–142, 2001.

Nirenberg MJ, Chan J, Pohorille A, Vaughan RA, Uhl GR, Kuhar MR, and Pickel VM. The dopamine transporter: comparative ultrastructure of dopaminergic axons in limbic and motor compartments of the nucleus accumbens. *J Neurosci* 17: 6899–6907, 1997.

Phillips PEM, Hancock PJ, and Stamford JA. Time window of autoreceptor-mediated inhibition of limbic and striatal dopamine release. *Synapse* 44: 15–22, 2002.

Phillips PEM, Stuber GD, Heien MLAV, Wightman RM, and Carelli RM. Subsecond dopamine release promotes cocaine seeking. *Nature* 422: 614–618, 2003.

Reiner A, Karle EJ, Anderson KD, and Medina L. Catecholaminergic perikarya and fibers in the avian nervous system. In: *Phylogeny and Development of Catecholaminergic Systems in the CNS of Vertebrates*, edited by Smeets WJAJ and Reiner A. Cambridge: Cambridge University Press, 1994, p. 135–181.

Reiner A, Perkel DJ, Bruce LL, Butler AB, Csillag A, Kuenzel W, Medina L, Paxinos G, Shimizu T, Striedter G, Wild M, Ball GF, Durand S, Güntürkün O, Lee DW, Mello CV, Powers A, White SA, Hough G, Kubikova L, Smulders TV, Wada K, Dugas-Ford J, Husband S, Yamamoto K, Yu J, Siang C, and Jarvis ED. Avian Brain Nomenclature Forum. Revised nomenclature for avian telenchephalon and some related brainstem nuclei. *J Comp Neurol* 473: 377–414, 2004.

Rice ME and Cragg SJ. Nicotine amplifies reward-releated dopamine signals in striatum. *Nat Neurosci* 7: 583–584, 2004.

Robinson DL, Heien MLAV, and Wightman RM. Frequency of dopamine concentration transients increases in dorsal and ventral striatum of male rats during introduction of conspecifics. *J Neurosci* 22: 10477–10486, 2002.

Robinson DL, Venton BJ, Heien MLAV, and Wightman RM. Detecting subsecond dopamine release with fast-scan cyclic voltammetry. *Clin Chem* 49: 1763–1773, 2003.

Roitman MF, Stuber GD, Phillips PEM, Wightman RM, and Carelli RM. Dopamine operates as a subsecond modulator of food seeking. *J Neurosci* 24: 1265–1271, 2004.

Scharff C and Nottebohm F. A comparative study of the behavioral deficits following lesions of various parts of the zebra finch song system: implications for vocal learning. *J Neurosci* 11: 2896–2913, 1991.

Schmitz Y, Benoit-Marand M, Gonon F, and Sulzer D. Presynaptic regulation of dopaminergic neurotransmission. *J Neurochem* 87: 273–289, 2003.

Schmitz Y, Lee JC, Schmauss C, Gonon F, and Sulzer D. Amphetamine distorts stimulation-dependent dopamine overflow: effects of D2 autoreceptors, transporters, and synaptic vesicle stores. *J Neurosci* 21: 5916–5924, 2001.

Schmitz Y, Schmauss C, and Sulzer D. Altered dopamine release and uptake kinetics in mice lacking D2 receptors. *J Neurosci* 22: 8002–8009, 2002.

Schultz W. Predictive reward signal of dopamine neurons. *J Neurophysiol* 80: 1–27, 1998.

Schroeter S, Apparsundaram S, Wiley RG, Miner LH, Sesack SR, and Blakely RD. Immunolocalization of the cocaine- and antidepressant-sensitive l-norepinephrine transporter. *J Comp Neurol* 420: 211–232, 2000.

Sesack SR, Hawrylak VA, Matus C, Guido MA, and Levey AI. Dopamine axon varicosities in the prelimbic division of the rat prefrontal cortex exhibit sparse immunoreactivity for the dopamine transporter. *J Neurosci* 18: 2697–2708, 1998.

Soha JA, Shimizu T, and Doupe AJ. Development of the catecholaminergic innervation of the song system of the male zebra finch. *J Neurobiol* 29: 473–489, 1996.

Sohrabji F, Nordeen EJ, and Nordeen KW. Selective impairment of song learning following lesions of a forebrain nucleus in the juvenile zebra finch. *Behav Neural Biol* 53: 51–63, 1990.

Stark LL and Perkel DJ. Two-stage, input-specific synaptic maturation in a nucleus essential for vocal production in the zebra finch. *J Neurosci* 19: 9107–9116, 1999.

Torres GE, Gainetdinov RR, and Caron MG. Plasma membrane monoamine transporters: structure, regulation and function. *Nat Rev Neurosci* 4: 13–25, 2003.

Trendelenburg A-U, Starke K, and Limberger N. Preynaptic α_{2a}-adrenoceptors inhibit the release of endogenous dopamine in rabbit caudate nucleus slices. *Nauyn-Schmiedeberg's Arch Pharmacol* 350: 473–481, 1994.

Venton BJ, Troyer KP, and Wightman RM. Response times of carbon fiber microelectrodes to dynamic changes in catecholamine concentration. *Anal Chem* 74: 539–546, 2002.

Yavich L, Lappalainen R, Sirvio J, Haapalinna A, and MacDonald E. α_2-Adrenergic control of dopamine overflow and metabolism in mouse striatum. *Eur J Pharmacol* 339: 113–119, 1997.

Williams H and Mehta N. Changes in adult zebra finch song require a forebrain nucleus that is not necessary for song production. *J Neurobiol* 39: 14–28, 1999.

Zhang W, Klimek V, Farley JT, Zhu M-Y, and Ordway GA. α_{2c} Adrenoceptors inhibit adenylyl cyclase in mouse striatum: potential activation by dopamine. *J Pharacol Exp Ther* 289: 1286–1292, 1999.

Zhang H and Sulzer D. Glutamate spillover in the striatum depresses dopaminergic transmission by activating group 1 metabotropic glutamate receptors. *J Neurosci* 22: 10585–10592, 2003.

Zhang H and Sulzer D. Frequency-dependent modulation of dopamine release by nicotine. *Nat Neurosci* 7: 581–582, 2004.

Zhou FM, Liang Y, and Dani JA. Endogenous nicotinic cholinergic activity regulates dopamine release in the striatum. *Nat Neurosci* 4: 1224–1229, 2001.